Research Article

Exposure to a Pathological Condition May Be Required for the Cells to Secrete Exosomes Containing mtDNA Aberration

Manjusha Vaidya, Sandeep Sreerama, Mariana Gaviria, and Kiminobu Sugaya [iD]

Burnett School of Biomedical Sciences, College of Medicine, University of Central Florida, Florida, USA

Correspondence should be addressed to Kiminobu Sugaya; ksugaya@ucf.edu

Exosomes, nanovesicles secreted by all cells, carry out intercellular communication by transmitting biologically active cargo comprising DNA, RNA, and proteins. These biomolecules reflect the status of their parent cells and can be altered by pathological conditions. Therefore, the researchers have been investigating differential sequences and quantities of DNA associated with exosomes as valuable biomarkers of diseases. Exosomes carry different types of DNA molecules, including genomic, cytoplasmic, and mitochondrial (mtDNA). The mtDNA aberrations are reported to be a hallmark of diseases involving oxidative stress, such as cancer and neurodegenerative diseases. Establishing robust *in vitro* models comprising appropriate cell lineages is the first step towards investigating disease-specific anomalies and testing therapeutics. Induced pluripotent stem (iPS) cells from patients with diseases have been used for this purpose since they can differentiate into various cells. The current study investigated mtDNA aberrations in exosomes secreted by primary cancer cells and neural stem cells (NSCs) differentiated from iPS cells. The primary cancer cells were isolated from surgically removed glioblastoma multiforme (GBM) tissue, and the iPS cells were produced from control and Alzheimer's disease (AD) subjects' B lymphocytes. We detected aberrations in mtDNA associated with exosomes secreted from GBM cells but not from the NSCs. This result indicates that the cells may not secrete exosomes carrying mtDNA aberration without exposure to a pathological condition. Thus, we may need to consider this fact when we use iPS cell-derived cells as an *in vitro* disease model.

1. Introduction

Exosomes are nanovesicles (30-130 nm) of late endocytic origin. Almost all types of cells secrete them for paracrine and endocrine intercellular communication (1). They can cross the blood-brain barrier (BBB) and anatomical compartments by transcytosis to be detected in peripheral blood and other body fluids (2). The exosome-associated DNA is found to carry disease-specific mutations as well as differential sequences resulting from disease progression and response to treatment. Mitochondrial DNA (mtDNA) in exosomes is a functionally active cargo. Its horizontal transfer to a new cell mediates hormonal therapy resistance in metastatic breast cancer, according to the research by Sansone et al. (3). Preexisting mutations of maternally inherited mtDNA are known to have clinical implications. On the other hand, it is well established that mtDNA is prone to

prolific damages such as mutation and degradation due to the lack of a robust repair mechanism, absence of histone-like protective proteins, and exposure to oxidants. Thus, the pathological cellular environment of a diseased cell is also known to cause changes in the mtDNA sequence (4, 5). Mitochondria are the ATP-generating powerhouses of a cell that utilize an oxidative phosphorylation system (OXPHOS). The crucial component proteins of OXPHOS subunits, except for subunit II, are encoded by genes in mtDNA. Therefore, mutations and differential sequences in mtDNA can be severely detrimental to cell function and survival (6). Impaired mitochondrial function and mutations in mtDNA are associated with many neurodegenerative diseases like Alzheimer's disease (AD) and cancers, including glioblastoma multiforme (GBM) (7–9). mtDNA alterations are useful as diagnostic and prognostic markers in liquid biopsy for GBM management (10). The mtDNA carrying

TABLE 1: PCR primers and their sequences used for exosomal mtDNA amplification.

Mitochondrial region	Location on NC_ 012920.1	Size (bp)	Primer pair [forward (F)/reverse (R)]	Reference
D-loop	321-496	175	F: 5′-TGGCCACAGCACTTAAACACATCTC-3′ R: 5′-GGGTTGTATTGATGAGATTAGTAGTATGG GAG-3′	(3)
16S ribosomal RNA	1873-2078	205	F: 5′-AACTTTGCAAGGAGAGCCAAAGC-3′ R: 5′-GGGATTTAGAGGGTTCTGTGGGC-3′	(3)
tRNA-Leu-UUR	3212-3319	107	F: 5′-CACCCAAGAACAGGGTTTGT-3′ R: 5′-TGGCCATGGGTATGTTGTTA-3′	(21, 22)
NADH dehydrogenase subunit 1	3458-3561	103	F: 5′-ACGCCATAAAACTCTTCACCAAAG-3′ R: 5′-TAGTAGAAGAGCGATGGTGAGAGCTA-3′	(23)

mutations is transported to adjacent cells via different modes, potentially creating a niche for the disease in a healthy cell, thereby contributing to disease pathology (11). Although mitochondria move to neighbor cells via tunneling nanotubes, mtDNA is known to migrate from one cell to another as an exosomal cargo. The population of mitochondria, the amount of DNA per mitochondrion, and the rate of DNA mutations vary depending on the disease. For example, mitochondria of various cancer cells possess more DNA coding for genes responsible for bioenergetics. Increased mtDNA copy numbers are reported in GBM differentiating cells and are associated with the initiation and maintenance of tumorigenesis (12–14). Antibiotic- or cancer-treatment-induced genotoxic shock may potentially send mtDNA to the exosome surface (13, 15). Radiation exposure is reported to elevate the mtDNA levels in exosomes secreted by human fibroblast cells (16). It is also reported that in the early stages of AD, the frequency of mtDNA mutations is remarkably high (7). These instances indicate that qualitative and quantitative changes in mtDNA are associated with the disease, its specific stage, progression, and response to therapy. Therefore, disease-specific modulations in exosome-associated mtDNA can serve as prognostic, diagnostic, and therapeutic intervention biomarkers. Analysis of mutations, single nucleotide polymorphisms (SNP), and deletions in the exosomal mtDNA secreted by cell lines cultured in vitro is an essential first step towards establishing their clinical validity.

2. Materials and Methods

2.1. Cell Culture. Human neural stem cells (NSC) were procured from Lonza (# PT2599). GBM cells were obtained from the resected mass of a tumor newly diagnosed via magnetic resonance imaging. The patient had not undergone GBM treatment earlier and had provided the Institutional Review Board-approved informed consent for the research study before the surgery. HIPPA regulations were strictly followed. A detailed characterization of these cell lines has been described in our previously published research (17). The tumor cells were dissociated for *in vitro* culture under the human subject protection protocol approved by

AdventHealth and the University of Central Florida Institutional Review Board. The cell lines were grown in suspension cultures in growth media comprising heparin 5000 U (0.5 U/ml), EGF 20 ng/ml, bFGF 20 ng/ml, and 2% B27 stock mixed in DMEM/F12. This suspension culture media does not require fetal bovine serum. Therefore, there is no interference of bovine exosomes. The induced pluripotent stem (iPS) cells derived from AD (iPS-AD) cell line were purchased from Coriell cell repositories (# CW50018). This cell line is reprogrammed from B lymphocytes of a subject diagnosed with AD. The diagnosis is based on the presence of Aβ peptide in the cerebrospinal fluid as well as affirmative ApoE4 carrier status (18). As a control for iPS-AD cells, iPS cells reprogrammed from B lymphocytes from a subject with no cognitive decline (iPS-control) were acquired from the Coriell cell repository (# CW50064). Following the protocol by Pauly et al., the iPS-control and iPS-AD cells were cultured to make iPS-derived neural stem cells (iPS-NSC and iPS-NSC-AD, respectively) (19). The conditioned media was collected for the isolation of exosomes after validation of neural stem cells by immunostaining and gene expression studies using SOX2, NESTIN, PAX6, and MSI1.

2.2. Exosome Isolation. The conditioned media of the cell cultures was centrifuged at $10,000 \times g$ for 30 minutes to remove cell remnants. The supernatant was transferred to a new tube, and 5 ml of 20% PEG and 200 μl of 7.5 M NaCl were added to each 10 ml volume to precipitate the exosomes (20). Upon overnight incubation at 4°C, the supernatant was centrifuged at $10,000 \times g$ for 60 minutes. The exosome pellet was resuspended in 1x PBS (pH 7.4, without calcium and magnesium). The manufacturer's protocol was followed to purify the exosomes further using CD63 antibody-conjugated magnetic beads (Thermo Fisher Scientific: Invitrogen Exosome Human CD63 Isolation/Detection Reagent (from cell culture media), Ref #10606D).

2.3. PCR Settings and Electrophoresis. Because this is a qualitative analysis, no exosomal DNA was extracted or quantified. Instead, a 15 μl exosomal suspension was used directly in place of the template for 50 μl PCR reaction volume. Using High-Performance GoTaq® G2 DNA Polymerase
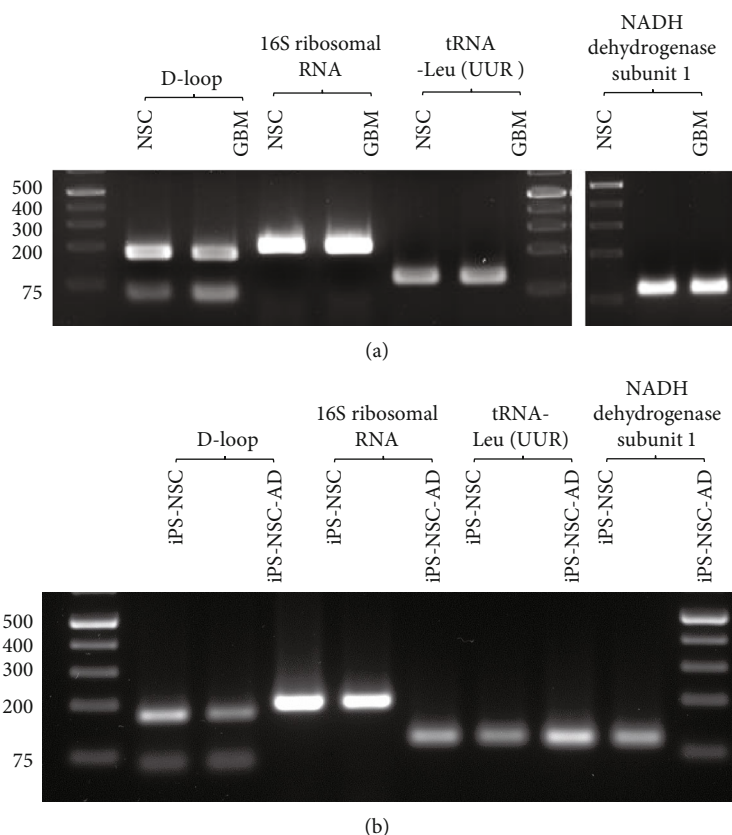
Figure 1: Typical gel images of exosomal mtDNA PCR products using primer sets described in Table 1. (a) NSC and GBM in the figure represent the mtDNA PCR products using exosomes isolated from neural stem cells (NSC) and glioblastoma multiforme (GBM) cell culture media as the sample. (b) iPS-NSC and iPS-NSC-AD in the figure represent the mtDNA PCR products using exosomes isolated from NSCs derived from iPS cells reprogrammed from B lymphocytes of control (iPS-NSC) and AD (iPS-NSC-AD) subjects.

(Promega) and mtDNA specific primer pairs (Table 1), the PCR reactions were set up as follows: 94°C—5 minutes (denaturation: 94°C—30 seconds, annealing: 50°C—30 seconds, extension: 72°C—2 minutes) × 30, 72°C—10 minutes. The PCR products were run on 1.5% agarose gel in 1x TAE buffer.

2.4. Cloning of PCR Products in pCR4TOPO-TA Vector. After gel electrophoresis of the PCR products, the DNA samples were eluted using QIAquick® Gel Extraction Kit (Qiagen, catalog # 28706) as per their protocol. Following the manufacturer's protocol, the PCR products were ligated with the pCR4TOPO-TA vector (Invitrogen™ TOPO™ TA Cloning™ Kit for Sequencing, catalog # 450030), transformed into chemically competent E. coli (*Stbl3*) cells, and selected on LB agar with ampicillin (100 μg/ml). Upon overnight incubation at 37°C, the colonies were picked, grown in LB with ampicillin, and the plasmid DNA was extracted using QIAprep Spin Miniprep Kit (QIAGEN #27104). On average, five clones for each PCR product-sequencing vector ligation were sent for Sanger sequencing with GENEWIZ®. With four cell lines and four primer pairs amplifying the mtDNA of a cell line, altogether, eighty clones were sent. The BLAST analysis of the clones is provided in the supple-

mentary section along with the four-color chromatograms showing the results of the respective sequencing runs Figures S-1–S-3.

2.5. Exosomal DNA Sequence Analysis. To eliminate the pCR4TOPO-TA vector sequences that could skew the analysis and the results, the nucleotide sequences received from GENEWIZ® were plugged into VacScreen from NCBI. Simultaneously, the forward and reverse primer sequences were identified, and the exact PCR product sequence was analyzed using the Basic Local Alignment Search Tool (BLAST). Standard BLAST search and human BLAST search were performed to investigate the identities of the PCR product. Exosomal mtDNA was also checked using the mtDNA-specific tool MITOMAP (https://http://www.MITOMAP.org/mitomaster/index.cgi). SNP found in the sequences was scrutinized for clinical significance using the NCBI SNP database.

2.6. Statistical Analysis. An ordinary two-way ANOVA was performed on the mean SNP number of each cell line per primer pair, followed by Tukey's multiple comparison test that compares individual differences. Software GraphPad Prism 9.3.0 was used to perform the analyses.
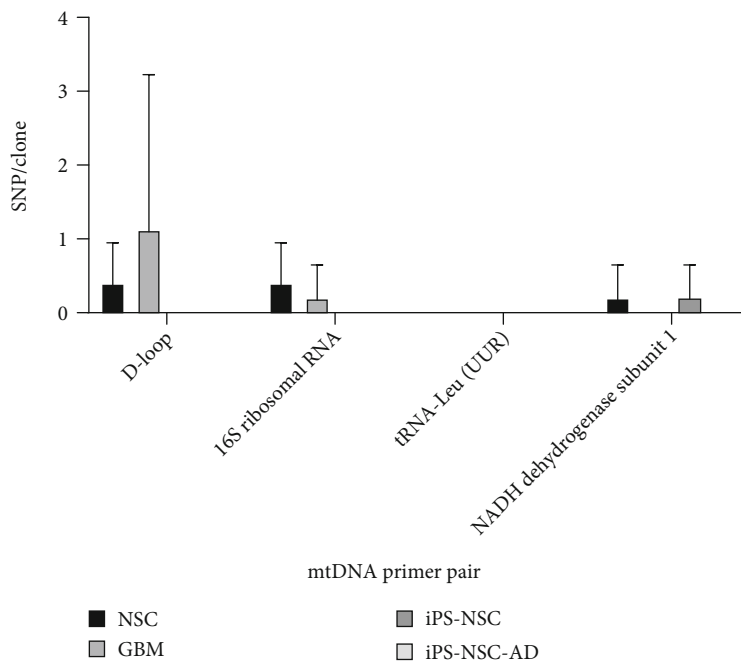
FIGURE 2: The number of the SNPs in clones obtained from the primer pair sets for D-loop, 16S ribosomal RNA, tRNA-Leu (UUR), and NADH dehydrogenase subunit 1 of mtDNA associated with exosomes released by neural stem cells (NSC), glioblastoma multiforme (GBM), control subject iPS-derived NSC (iPS-NSC), and AD subject iPS cells (iPS-NSC-AD). The numbers of SNPs in each group ($n = 5$) are presented as mean ± SD. Two-way ANOVA followed by Tukey's multiple comparison *post hoc* analysis was performed, and there was no significant difference among the groups ($P > 0.05$).

3. Results

The current study is aimed at investigating whether the iPS cell-based *in vitro* disease model can reproduce the exosomal mtDNA aberrations resulting from a cellular environment changed by the disease. We hypothesized that cells exposed to the disease would secrete exosomes with variations in mtDNA sequence because of the stress generated by the disease pathology. Therefore, exosomal mtDNA secreted by iPS-AD derived from peripheral tissue, which has never been exposed to a pathological condition, such as oxidative stress, may not have any variations in the mtDNA sequence. As the diseased models, we used primary cells from GBM tissue and the NSCs derived from iPS-AD. As the controls, we used fetal NSCs and NSCs derived from iPS cells of healthy subjects. We analyzed the specific regions of exosomal mtDNA, reported to show differential sequences in these diseases (3, 21–23) for the clonal variations of nucleotides and SNPs. This approach may help amplify and analyze the specific region of mtDNA sequence in the exosome because it may be randomly fragmented and complex to sequence the entire mitochondria genome by next-generation sequencing. Also, identifying new molecular markers for these diseases is not the purpose of this study.

We used primer sets to amplify the specific region of mtDNA, which are reported to be associated with these diseases, namely, D-loop, 16S ribosomal RNA, tRNA-Leu-UUR, and NADH dehydrogenase subunit 1, which are described in Table 1. Figure 1 shows a typical gel electrophoresis image of amplified exosomal mtDNA.

In two-way ANOVA, the SNP analysis of each clone for all the cell types tested and primer pair showed a slight variation with no statistical significance (Figure 2). However, in-depth BLAST analysis of the clone obtained with each primer pair revealed SNPs in GBM cells, underscoring the heteroplasmy in exosomal mtDNA. The BLAST analysis of the clones and the SNPs and their MITOMAP reports are discussed in detail in the following section.

3.1. Displacement Loop (D-loop) 321-496. BLAST analysis revealed that PCR primers amplified the expected regions of mtDNA associated with GBM and iPS-NSC-AD exosomes and the mtDNA of their normal counterparts. While NSC exosomes had barely one SNP per clone in two of the clones ($n = 2$) (Figure 3), BLAST analysis has identified over 9 SNP together in two clones of GBM exosomal mtDNA ($n = 9$). Where four-color chromatograms show the results of the sequencing run, the red arrows point to the SNPs (Supplementary Figures S-4 and S-5). These SNPs are listed in Table 2. Where some of these SNPs are reported in the MITOMAP database, others are novel. This finding supports the research that the D-loop region is prime for point mutations and SNP with pathogenic relevance to GBM (5, 24). Out of three highly polymorphic hypervariable segments of D-loop (HVI: 16024–16383, HVII: 57–372, and HVIII: 438–574), we have partially amplified regions II and III (321-496). Although most SNP is also reported in MITOMAP, their presence in GBM exosomal DNA is significant. Not only in gliomas and other types of cancers, D-loop mutations and SNP are also

BLAST ® » blastn suite-2sequences » RID-HNCFWUHW114
Homo sapiens mitochondrion, complete genome
Sequence ID: gi|251831106|NC_012920.1Length: 16569Number of Matches: 1

Range 1: 321 to 496 GenBank Graphics
Alignment statistics for match #1
Score Expect Identities   Gaps   Strand
310 bits(343) 2e-87 175/176(99%) 1/176(0%)   Plus/Minus

```
Query  1    GGGTTGTATTGATGAGATT-GTAGTATGGGAGTGGGAGGGGAAAATAATGTGTTAGTTGG  59
            |||||||||||||||||||| |||||||||||||||||||||||||||||||||||||||
Sbjct  496  GGGTTGTATTGATGAGATTAGTAGTATGGGAGTGGGAGGGGAAAATAATGTGTTAGTTGG  437

Query  60   GGGGTGACTGTTAAAAGTGCATACCGCCAAAAGATAAAATTTGAAATCTGGTTAGGCTGG  119
            ||||||||||||||||||||||||||||||||||||||||||||||||||||||||||||
Sbjct  436  GGGGTGACTGTTAAAAGTGCATACCGCCAAAAGATAAAATTTGAAATCTGGTTAGGCTGG  377

Query  120  TGTTAGGGTTCTTTGTTTTTGGGGTTTGGCAGAGATGTGTTTAAGTGCTGTGGCCA  175
            ||||||||||||||||||||||||||||||||||||||||||||||||||||||||
Sbjct  376  TGTTAGGGTTCTTTGTTTTTGGGGTTTGGCAGAGATGTGTTTAAGTGCTGTGGCCA  321
```

(a)
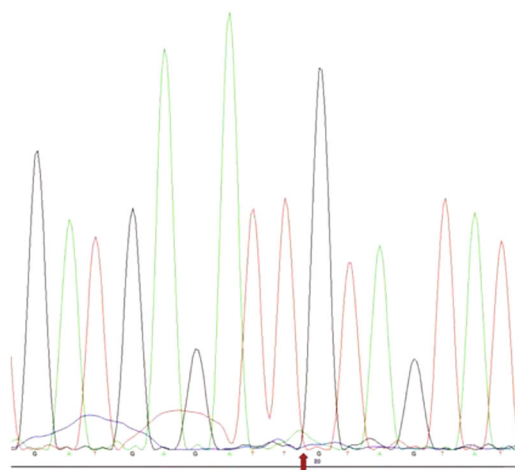
(b)

rCRS position	Query position	rCRS NT	Query NT	Mut type	Locus	Other	GB Freq FL (CR)*‡	GB Seqs FL (CR)*	Freq % in H2a	Conservation
477	157	T	:	deletion	CR:HVS3	non-coding	0.00%	0 (0)	0.000 (0/808)	NA
					ATT CR:Control region		0.00%			

(c)

FIGURE 3: NSC exosome D-loop clone. (a) BLAST analysis against *Homo sapiens* mitochondrion, complete genome NC_012920.1. CD63+ exosomal mtDNA amplified with D-loop primers (location: 321-496). PCR products were cloned into the pCR4-TOPO-TA vector. (b) The red arrow in the sequence figure indicates the position of the nucleotide deletion in exosomal DNA in *Homo sapiens* mitochondrion complete genome sequence (NC_012920.1). The entire chromatogram of the clone is provided in the supplementary section (Figure S-7). (c) Singular SNP at 477 (A>-) found in the clone (bold letter in (a)) is also reported in MITOMAP at rCRS position 477 (T>-). Information from MITOMAP: *the current GB frequency data is derived from two sets of human mitochondrial sequences from GenBank: 52,633 full-length (FL) sequences (>15.4 kbp) and 74,970 short, control region (CR) containing sequences (0.4-1.6 kbp); ‡high-frequency haplogroups: variants found in haplogroups at 50% or higher are marked with a flag.

reported in AD [7]. For the amplified D-loop region 321-496, we did not find any SNP or mutations in the iPS-NSC-AD exosomes (Supplementary Figure S-6). An effect of aging, nucleotide variations accumulate in mtDNA, including the highly susceptible D-loop region, and the donor's age for iPSC-AD B-lymphocytes used in our study was 58 years, old enough to have possible nucleotide differences in the mtDNA sequence [25]. Additionally, mutation load is reported to be significantly higher in neuronal mitochondria in AD [7]. Although the B

TABLE 2: A concise account of the SNP found in exosomal mtDNA. D-loop region 321-496 in GBM has a significantly higher occurrence of SNP over other regions and cell lines. Except for one SNP found at position 3545 (C>-) in NADH dehydrogenase subunit 1 region 3458-3561, the rest of the iPS-NSC and iPS-NSC-AD cell line clones had 100% identity to the reported sequences in the human mitochondrial genome (NC_012920.1) for all other genes. Each SNP in a clone is unique irrespective of the primer pair or a cell line.

Exosomal cell source	mtDNA region	Position on NC_012920.1	SNP
NSC	D-loop	321-496	477 A>-, 334 T>-
GBM	D-loop	321-496	371 G>N, 426 T>A, 420 G>N, 404 G>T, 481: G>N, 480: A>T, 478: T>N, 477: A>N and 379: T>C, 480: T>A
NSC	16S ribosomal RNA	1873-2078	1893 A>-, 1900 T>C
GBM	16S ribosomal RNA	1873-2078	1884 C>-
GBM	tRNA-Leu-UUR	3212-3319	None
NSC	tRNA-Leu-UUR	3212-3319	None
NSC	NADH dehydrogenase subunit 1	3458-3561	3502, T>A
iPS-NSC	NADH dehydrogenase subunit 1	3458-3561	3545 C>-

lymphocyte donor was diagnosed with the disease, the mtDNA in exosomes did not reflect the mutations.

3.2. 16S Ribosomal RNA (16S mt-rRNA) 1873-2078. The clones analyzed for regions 1873-2078 have shown very few nucleotide variations irrespective of the cell source and disease. GBM exosomal PCR products showed a novel deletion at 1884 C>-, which has not been reported in MITOMAP. Two different clones of NSC exosomal DNA had two SNPs per clone. Where SNP at 1893 (A>-) is novel, SNP at 1900 T>C is reported in MITOMAP (Table 2). Elson et al. have reported several nucleotide variations and mutations in 16S mt rRNA that can disrupt the activity of the small ribosomal subunit and have implications in various cancers (26). We did not find any of these SNP in the region amplified.

3.3. tRNA-Leu (UUR) 3212-3319. In the tRNA-Leu (UUR) region, a transition type of pathogenic mutation found in mt-tRNA-Leu (UUR) at 3243 A>G is most frequent in humans. It is associated with mitochondrial encephalopathy, lactic acidosis, stroke-like episodes, and diabetes (27, 28). It is also reported that the tRNA-Leu (UUR) region is a prime spot for pathogenic mtDNA mutations (29). In our study, neither GBM/NSC nor iPSC-NSC/iPSC-NSC-AD showed any SNP in the exosomal mtDNA for region 3212-3319 of tRNA-Leu (UUR).

3.4. NADH Dehydrogenase Subunit 1 (ND1) 3458-3561. Where NSC-derived exosomes had one SNP at 3502 T>A (also reported in MITOMAP), GBM PCR products matched 100% with the human mitochondrial genome (NC_012920.1). Similarly, iPS-NSC had single and novel SNP at 3545 (C>-) not reported in MITOMAP (Table 2). In MITO-MAP, an SNP is reported at 3546 (C>-) with a frameshift. Mutations in ND1 are implicated in colorectal carcinoma, hepatocellular carcinoma, and human gastric cancer, and SNP in this mtDNA gene is studied as a potential risk factor for breast cancer (30–33). In addition, mutations in this

mitochondrial gene have prognostic value in postoperative renal cell carcinoma (34).

4. Discussion

Unlike nuclear DNA, mtDNA undergoes fewer epigenetic changes. For example, methylation of the D-loop region is crucial in neurodegenerative diseases and cancers alike. Although methylation levels of mtDNA are significantly lower than nuclear DNA, this type of regulation has a potential role in replicating mtDNA and transcription of genes. Mutations in D-loop can compromise its methylation status (35). In a clustered data analysis, GBM clones do not show significant variation in the mean value. However, when the nucleotide variants are present in a clone, their frequency is higher in the D-loop region, known for elevated susceptibility to mutations. Yeung et al. have also checked the D-loop in cultured NSC to see the effect of culture conditions on nucleotide variation in this region. They detected two variations, the same amount found in NSC exosomal mtDNA, although at different nucleotides in the sequence (9). This underscores the importance of the D-loop region's differential sequences found in the exosomes of GBM. The same research group has also reported that some mtDNA-coding regions such as ND1 are unaffected in GBM. They found no variants in this gene. Our GBM exosomal mtDNA clones do not have any SNP either. This finding agrees with their data suggesting that the lack of mtDNA variation at the source reflects the SNP-devoid status in exosomal mtDNA.

Like GBM, neuronally extracted mtDNA with Alzheimer's pathology has shown significantly elevated mutations in the D-loop (7). Hoekstra et al. have demonstrated that the mutation load in this noncoding D-loop region is many folds higher than that in the coding region. This ratio is independent of the AD condition. However, in our study, the iPSC-NSC-AD exosomes had 100% identity to the reported sequence and no SNP. Although the donor was diagnosed with AD as described before, the iPSCs were created using B lymphocytes, which lacked AD pathology

found in neural cells and mitochondria. In particular, the sporadic change in mtDNA is highly dependent on the environment. Thus, the iPS cell-derived exosomal mtDNA may have failed to reflect the sequence and nucleotide variations attributed to degeneration or pathological changes in neural cells. This indicates that although the researchers have successfully established iPS-derived neuronal models to study AD as well as other neurodegenerative diseases and established mtDNA as one of the disease biomarkers, iPS model-derived exosomal mtDNA may not be ideal for the biomarker studies (36, 37).

In addition to the primers described in Table 1, other regions of exosomal mtDNA were amplified by PCR. However, the PCR for NADH, DHG-sub2, ATP-6, MTCYB, 12S ribosomal RNA, and an 8842-nucleotide long fragment (position 5999-14841) did not yield any product. However, all the primer sets successfully amplified the target genes when cytoplasmic DNAs were used as templates, indicating that mtDNAs associated with exosomes are fragmented. Fragmented mtDNAs are reported to be released from defective mitochondria during their turnover and hauled away for clearance by exosomes and other extracellular vesicles (38).

5. Conclusions

Only the exosomal mtDNA from GBM cells showed aberrations as reported by other researchers in these specific regions, while the exosomal mtDNA from fetal NSCs and iPS-derived NSCs were almost identical to the sequences reported in GenBank. The GBM cells are derived from a resected tumor tissue, and they are directly exposed to the disease environment. The iPS-NSC-AD cells, which are reprogrammed from B lymphocytes, are not subjected to AD pathology, although it has been differentiated in NSCs. Thus, exposure to the pathological environments may be needed for the cells to secrete exosomes that carry mtDNA aberrations. The cell culture model based on the specific cell linage derived from iPS cells, which has been used to investigate many diseases, may fall short of reproducing the disease-related intracellular environments, which reflect the exosomal mtDNA. In order to avoid this issue, we may need to use primary neural cells directly from the patient's brain to investigate the effect of AD pathology in some cases. Another note is that we did not detect the difference in exosomal mtDNA sequence secreted by primary NSC, iPS-NSC-AD, and iPS-NSC cells. This may indicate that reprograming process to produce iPS cells may not affect mtDNA sequence.

Data Availability

No data were used to support this study.

Ethical Approval

The study was conducted according to the guidelines of The Privacy Rule issued under a law called the Health Insurance Portability and Accountability Act of 1996 (HIPAA) and approved by the Institutional Review Board of University of Central Florida, STUDY00001525; date: Monday, November 2, 2020, 9:23:36 AM.

Consent

Prior to enrollment to the study, informed consent was obtained from each patient participating in the clinical trial. The informed consent was compliant with applicable federal regulations (including FDA 21 CFR 50.20-50.27 and DHHS 45 CFR 46) and approved by AdventHealth and University of Central Florida Institutional Review Boards (IRB).

Conflicts of Interest

The authors have no conflict of interest to declare.

Authors' Contributions

M.V. and K.S. were responsible for conceptualization; M.V., S.S., and M.G. were responsible for investigation; K.S. was responsible for resources; K.S. was responsible for data curation; M.V. was responsible for writing—original draft preparation; K.S. was responsible for writing—review and editing; M.V. and K.S. were responsible for visualization; K.S. was responsible for supervision; K.S. was responsible for project administration; K.S. was responsible for funding acquisition. All authors have read and agreed to the published version of the manuscript.

Acknowledgments

Supplementary Materials

Figure S-1: human BLAST analysis of the exosomal mtDNA clones. PCR product was obtained using 16S ribosomal RNA primers that amplify region 1873-2078 (Homo sapiens mitochondrion, complete genome NC_012920.1). The amplification product was ligated with Invitrogen™ pCR4TOPO-TA sequencing vector. The clones were selected on ampicillin and Sanger sequenced by GENEWIZ®. The sequences are analyzed using the Basic Local Alignment Search Tool (BLAST). SNPs are highlighted by a red rectangle. (A) NSC exosomes: SNP @ 1893 A>-. (B) GBM exosomes: deletion/SNP @ 1884 C>-. (C) iPS-NSC and iPS-NSC-AD have 100% sequence identity with each other as well as with mitochondrial genomic sequence and no SNP. Figure S-2: human BLAST analysis of the exosomal mtDNA clones. PCR product obtained using tRNA-Leu (UUR) primers that amplify region 3212-3319 (Homo sapiens mitochondrion, complete

genome NC_012920.1). The amplification product was ligated with Invitrogen™ pCR4TOPO-TA sequencing vector. The clones were selected on ampicillin and Sanger sequenced by GENEWIZ®. The sequences are analyzed using the Basic Local Alignment Search Tool (BLAST). NSC, GBM, iPS-NSC, and iPS-NSC-AD exosomal clones share 100% identity with each other as well as with mitochondrial genomic sequence. Figure S-3: human BLAST analysis of the exosomal mtDNA clones. PCR product obtained using NADH dehydrogenase subunit 1 primers that amplify region 3458-3561 (Homo sapiens mitochondrion, complete genome NC_012920.1). The amplification product was ligated with Invitrogen™ pCR4TOPO-TA sequencing vector. The clones were selected on ampicillin and Sanger sequenced by GENEWIZ®. The sequences are analyzed using the Basic Local Alignment Search Tool (BLAST). SNPs are highlighted by a red rectangle. (A) NSC exosomes: SNP @ 3502, T>A. (B) iPS-NSC exosomes: SNP @ 3545 C>-. (C) GBM and iPS-NSC-AD exosomes have 100% sequence identity with each other as well as with mitochondrial genomic sequence and no SNP. Figure S-4: GBM exosome D-loop clone 1. (A) BLAST analysis against Homo sapiens mitochondrion, complete genome NC_012920.1: CD63+ exosomal mtDNA was amplified with D-loop primers (location: 321-496). PCR products were cloned into the pCR4-TOPO-TA vector. SNPs at 371 G>N, 426 T>A, 420 G>N, and 404 G>T. (B) rCRS position according to MITOMAP: at 404: C>A, at 426: A>T, mutation type transversion. Information from MITOMAP: *the current GB frequency data is derived from two sets of human mitochondrial sequences from GenBank: 52,633 full-length (FL) sequences (>15.4 kbp) and 74,970 short, control region (CR) containing sequences (0.4-1.6 kbp); ‡high-frequency haplogroups: variants found in haplogroups at 50% or higher are marked with a flag. (C) The chromatogram depicts the sequence of the entire PCR product cloned. The red arrows correspond to the SNPs. Figure S-5: GBM exosome D-loop clone 2. (A) BLAST analysis against Homo sapiens mitochondrion, complete genome NC_012920.1. CD63+ exosomal mtDNA was amplified with D-loop primers (location: 321-496). PCR products were cloned into the pCR4-TOPO-TA vector. SNPs at 481: G>N, 480: A>T, 478: T>N, 477: A>N, and 379: T>C. (B) rCRS positions according to MITOMAP: @379: A>G (mutation type: transition), at 480: T>A, (mutation type transversion). Information from MITOMAP: *the current GB frequency data is derived from two sets of human mitochondrial sequences from GenBank: 52,633 full-length (FL) sequences (>15.4 kbp) and 74,970 short, control region (CR) containing sequences (0.4-1.6 kbp); ‡high-frequency haplogroups: variants found in haplogroups at 50% or higher are marked with a flag. (C) Because the clone has identical sequence to the one in Figure S-4, except for the SNPs, the chromatogram shows only the unique SNPs here, marked by a red arrow. Figure S-6: (A) iPS-NSC exosomes and (B) iPS-NSC-AD exosomes, D-loop clones. BLAST analysis against Homo sapiens mitochondrion, complete genome NC_012920.1. CD63+ exosomal mtDNA was amplified with D-loop primers (location: 321-496). PCR products were cloned

into the pCR4-TOPO-TA vector. With 100% identity to the reported sequences, there are no SNPs in this region. (C) The chromatogram depicts the sequence of the entire PCR product cloned. Figure S-7: human BLAST analysis of the exosomal mtDNA NSC exosome D-loop clone. A detailed chromatogram for Figure 3(b). PCR product was obtained using D-loop RNA primers that amplify region 321-496 (Homo sapiens mitochondrion, complete genome NC_012920.1). The amplification product was ligated with Invitrogen™ pCR4TOPO-TA sequencing vector. The clones were selected on ampicillin and Sanger sequenced by GENEWIZ®. The sequences are analyzed using the Basic Local Alignment Search Tool (BLAST). The red arrow in the sequence figure indicates the position of the nucleotide deletion in exosomal DNA in Homo sapiens mitochondrion complete genome sequence (NC_012920.1). *(Supplementary materials)*

References

[1] J. R. Edgar, "Q&A: what are exosomes, exactly," *BMC Biology*, vol. 14, no. 1, pp. 1–7, 2016.

[2] W. A. Banks, P. Sharma, K. M. Bullock, K. M. Hansen, N. Ludwig, and T. L. Whiteside, "Transport of extracellular vesicles across the blood-brain barrier: brain pharmacokinetics and effects of inflammation," *International journal of molecular sciences.*, vol. 21, no. 12, p. 4407, 2020.

[3] P. Sansone, C. Savini, I. Kurelac et al., "Packaging and transfer of mitochondrial DNA via exosomes regulate escape from dormancy in hormonal therapy-resistant breast cancer," *Proceedings of the National Academy of Sciences*, vol. 114, no. 43, pp. E9066–E9075, 2017.

[4] M. Paraskevaidi, P. L. Martin-Hirsch, M. Kyrgiou, and F. L. Martin, "Underlying role of mitochondrial mutagenesis in the pathogenesis of a disease and current approaches for translational research," *Mutagenesis*, vol. 32, no. 3, pp. 335–342, 2017.

[5] D. C. Wallace, "Mitochondria and cancer," *Nature Reviews Cancer.*, vol. 12, no. 10, pp. 685–698, 2012.

[6] M. Pinto and C. T. Moraes, "Mitochondrial genome changes and neurodegenerative diseases," *Biochimica et Biophysica Acta (BBA)-Molecular Basis of Disease.*, vol. 1842, no. 8, pp. 1198–1207, 2014.

[7] J. G. Hoekstra, M. J. Hipp, T. J. Montine, and S. R. Kennedy, "Mitochondrial DNA mutations increase in early stage Alzheimer disease and are inconsistent with oxidative damage," *Annals of Neurology*, vol. 80, no. 2, pp. 301–306, 2016.

[8] O. Russell and D. Turnbull, "Mitochondrial DNA disease–molecular insights and potential routes to a cure," *Experimental cell research.*, vol. 325, no. 1, pp. 38–43, 2014.

[9] K. Y. Yeung, A. Dickinson, J. F. Donoghue et al., "The identification of mitochondrial DNA variants in glioblastoma multiforme," *Acta neuropathologica communications*, vol. 2, no. 1, pp. 1–21, 2014.

[10] M. B. Leão Barros, D. R. Pinheiro, and B. N. Borges, "Mitochondrial DNA alterations in glioblastoma," *International Journal of Molecular Sciences*, vol. 22, no. 11, p. 5855, 2021.

[11] L. Isola and A, Chen S, "Exosomes: the messengers of health and disease," *Current Neuropharmacology*, vol. 15, no. 1, pp. 157–165, 2017.

[12] J. B. Stewart and P. F. Chinnery, "The dynamics of mitochondrial DNA heteroplasmy: implications for human health and disease," *Nature Reviews Genetics.*, vol. 16, no. 9, pp. 530–542, 2015.

[13] C. Kahlert, S. A. Melo, A. Protopopov et al., "Identification of double-stranded genomic DNA spanning all chromosomes with mutated _KRAS_ and _p53_ DNA in the serum exosomes of patients with pancreatic cancer*," *Journal of Biological Chemistry*, vol. 289, no. 7, pp. 3869–3875, 2014.

[14] A. Dickinson, K. Yeung, J. Donoghue et al., "The regulation of mitochondrial DNA copy number in glioblastoma cells," *Cell Death & Differentiation*, vol. 20, no. 12, pp. 1644–1653, 2013.

[15] A. Németh, N. Orgovan, B. W. Sódar et al., "Antibiotic-induced release of small extracellular vesicles exosomes with surface-associated DNA," *Scientific Reports*, vol. 7, no. 1, pp. 1–16, 2017.

[16] K. Ariyoshi, T. Miura, K. Kasai, Y. Fujishima, A. Nakata, and M. Yoshida, "Radiation-induced bystander effect is mediated by mitochondrial DNA in exosome-like vesicles," *Scientific Reports*, vol. 9, no. 1, pp. 1–14, 2019.

[17] A. A. Alvarez, M. Field, S. Bushnev, M. S. Longo, and K. Sugaya, "The effects of histone deacetylase inhibitors on glioblastoma-derived stem cells," *Journal of Molecular Neuroscience*, vol. 55, no. 1, pp. 7–20, 2015.

[18] F. Iannuzzi, R. Sirabella, N. Canu, T. J. Maier, L. Annunziato, and C. Matrone, "Fyn tyrosine kinase elicits amyloid precursor protein Tyr682 phosphorylation in neurons from Alzheimer's disease patients," *Cell*, vol. 9, no. 8, p. 1807, 2020.

[19] M. G. Pauly, V. Krajka, F. Stengel, P. Seibler, C. Klein, and P. Capetian, "Adherent vs. free-floating neural induction by dual SMAD inhibition for neurosphere cultures derived from human induced pluripotent stem cells," *Frontiers in Cell and Developmental Biology*, vol. 6, p. 3, 2018.

[20] M. A. Rider, S. N. Hurwitz, and D. G. Meckes Jr., "ExtraPEG: a polyethylene glycol-based method for enrichment of extracellular vesicles," *Scientific Reports*, vol. 6, no. 1, p. 23978, 2016.

[21] V. Venegas and M. C. Halberg, "Measurement of mitochondrial DNA copy number," *Methods Mol Biol*, vol. 837, pp. 327–335, 2012.

[22] V. Venegas and M. C. Halberg, "Quantification of mtDNA mutation heteroplasmy ARMS qPCR," in *Mitochondrial Disorders*, pp. 313–326, Springer, 2012.

[23] M. Guescini, S. Genedani, V. Stocchi, and L. F. Agnati, "Astrocytes and glioblastoma cells release exosomes carrying mtDNA," *Journal of Neural Transmission*, vol. 117, no. 1, pp. 1–4, 2010.

[24] A. A. Mohamed Yusoff, K. N. Mohd Nasir, K. Haris et al., "Detection of somatic mutations in the mitochondrial DNA control region D-loop in brain tumors: the first report in Malaysian patients," *Oncology letters.*, vol. 14, no. 5, pp. 5179–5188, 2017.

[25] M. T. Lin, D. K. Simon, C. H. Ahn, L. M. Kim, and M. F. Beal, "High aggregate burden of somatic mtDNA point mutations in aging and Alzheimer's disease brain," *Human molecular genetics.*, vol. 11, no. 2, pp. 133–145, 2002.

[26] J. L. Elson, P. M. Smith, L. C. Greaves et al., "The presence of highly disruptive 16S rRNA mutations in clinical samples indicates a wider role for mutations of the mitochondrial ribosome in human disease," *Mitochondrion*, vol. 25, pp. 17–27, 2015.

[27] Y. Kobayashi, M. Y. Momoi, K. Tominaga et al., "A point mutation in the mitochondrial tRNA^{Leu}(UUR) gene in melas (mitochondrial myopathy, encephalopathy, lactic acidosis and stroke- like episodes)," *Biochemical and biophysical research communications.*, vol. 173, no. 3, pp. 816–822, 1990.

[28] R. Li and M.-X. Guan, "Human mitochondrial leucyl-tRNA synthetase corrects mitochondrial dysfunctions due to the tRNALeu (UUR) A3243G mutation, associated with mitochondrial encephalomyopathy, lactic acidosis, and stroke-like symptoms and diabetes," *Molecular and cellular biology.*, vol. 30, no. 9, pp. 2147–2154, 2010.

[29] K. Maniura-Weber, M. Helm, K. Engemann et al., "Molecular dysfunction associated with the human mitochondrial 3302A> G mutation in the MTTL1 (mt-tRNALeu (UUR)) gene," *Nucleic acids research.*, vol. 34, no. 22, pp. 6404–6415, 2006.

[30] Y. Yusnita, M. D. Norsiah, and A. J. Rahman, "Mutations in mitochondrial NADH dehydrogenase subunit 1 (mtND1) gene in colorectal carcinoma," *The Malaysian journal of pathology.*, vol. 32, no. 2, pp. 103–110, 2010.

[31] P.-H. Yin, C.-C. Wu, J.-C. Lin, C.-W. Chi, Y.-H. Wei, and H.-C. Lee, "Somatic mutations of mitochondrial genome in hepatocellular carcinoma," *Mitochondrion*, vol. 10, no. 2, pp. 174–182, 2010.

[32] W.-Y. Hung, C.-W. Wu, P.-H. Yin et al., "Somatic mutations in mitochondrial genome and their potential roles in the progression of human gastric cancer," *Biochimica et Biophysica Acta (BBA)-General Subjects.*, vol. 1800, no. 3, pp. 264–270, 2010.

[33] A. M. Czarnecka, A. Klemba, T. Krawczyk et al., "Mitochondrial NADH-dehydrogenase polymorphisms as sporadic breast cancer risk factor," *Oncology reports.*, vol. 23, no. 2, pp. 531–535, 2010.

[34] H. Kim, T. Komiyama, C. Inomoto et al., "Mutations in the mitochondrial ND1 gene are associated with postoperative prognosis of localized renal cell carcinoma," *International journal of molecular sciences.*, vol. 17, no. 12, p. 2049, 2016.

[35] F. Coppedè and A. Stoccoro, "Mitoepigenetics and neurodegenerative diseases," *Frontiers in endocrinology.*, vol. 10, p. 86, 2019.

[36] A. Picca, F. Guerra, R. Calvani et al., "Mitochondrial-derived vesicles as candidate biomarkers in Parkinson's disease: rationale, design and methods of the EXosomes in PArkiNson Disease (EXPAND) study," *International journal of molecular sciences.*, vol. 20, no. 10, p. 2373, 2019.

[37] K. E. Hawkins and M. Duchen, "Modelling mitochondrial dysfunction in Alzheimer's disease using human induced pluripotent stem cells," *World journal of stem cell.*, vol. 11, no. 5, pp. 236–253, 2019.

[38] S. Srivastava and K. Morris, "The multifunctionality of exosomes; from the garbage bin of the cell to a next generation gene and cellular therapy," *Genes*, vol. 12, no. 2, p. 173, 2021.